esting that both the computational method of "coarse particles" and the approximate CCW theory, which is somewhat formally used in this problem, are handled mainly with functions to describe shock interaction with a permeable obstacle in a homogeneous approximation.

LITERATURE CITED

1. V. G. Dulov, "Decay of an arbitrary discontinuity of gas parameters by a jump of the section area," Vestn. Leningr. Univ., No. 14, Issue 4 (1958).
2. Yu. P. Il'in, "Shock interaction with pliable and permiable bodies," Candidate's Dissertation, Physico-mathematical Sciences, Leningrad Polytech. Inst. (1979).
3. E. F. Zhigalko, "Simplest solutions of problems on shock interaction with permeable walls," Uch. Zap. Leningrd. Univ., Gazodin. Teploobmen., No. 4 (1975).
4. R. F. Chisnell, "The motion of a shock wave in a channel with applications to cylindrical and spherical shock waves," J. Fluid Mech., No. 2 (1957).
5. R. A. Mortin, R. E. Gentry, and B. J. Daly, "An Eulerian differencing method for unsteady compressible flow problems," J. Comp. Phys., No. 1 (1966).
6. O. M. Belotserkovskii and Yu. M. Davydov, "Computation of transsonic 'post-critical' flow regimes by the method of 'coarse particles'," Vychisl. Mat. Mat. Fiz., 13, No. 1 (1973).

REGIMES AND PROPERTIES OF THREE-DIMENSIONAL SEPARATION FLOWS INITIATED BY SKEWED COMPRESSION SHOCKS

A. A. Zheltovodov

UDC 532.526.5

The study of singularities in the three-dimensional interaction between an oblique compression shock and the boundary layer on a plane surface normal to the plane of the shock and parallel to the free-stream velocity vector is quite important to the comprehension of regularities in the origination and development of three-dimensional separation flows.

Sufficiently extensive information about the different properties of the flows under consideration is contained in published papers. Thus an analysis is made in [1] of known data on the three-dimensional interaction between an oblique shock and laminar and turbulent boundary layers. The results in this paper, together with [2], yield a representation of the flow structure at different stages of the interaction, from the start of separation into return flow. Correlation relationships are obtained to determine conditions for the origination of the separation flow [3] and the formation of secondary separation [4], as well as for the computation of the characteristic pressures and heat fluxes in the separation zones [5]. Measurements of the fields of different parameters are performed in the interaction domain [6].

Systematic investigations of the dynamics of separation flow development and its structure [7, 8] should especially be noted, which radically extend existing representations of its properties and refine the phenomenological schemes proposed earlier. The possibility and development of a secondary separation zone of bounded extent is detected in the last two papers. It is shown that there is no secondary separation under these conditions in the return stream in the turbulent boundary layer domain, and the increae in its extent in the laminar flow domain as the shock intensity grows is related to fastening the transition because of the intensifying spread of the flow, which contributes to diminution of the return flow streamline extent. The analysis performed in these papers also permitted showing that the disappearance detected in [9] and the repeated origination of the secondary separation for sufficiently high shock intensities is associated with the transformation of conically subsonic into supersonic flow in the separation zone. An important deduction is made here that the duplicate origination of secondary flow should be determined by the state of the boundary layer in the return flow and by the intensity of the internal compression shock which will occur.

In order to refine further the features of oblique compression shock interaction with a turbulent boundary layer being developed on a flat surface (Fig. 1), experimental investigations are performed for the Mach num-

Novosibirsk. Translated from Zhurnal Prikladnoi Mekhaniki i Tekhnicheskoi Fiziki, No. 3, pp. 116-123, May-June, 1982. Original article submitted May 22, 1981.

0021-8944/82/2303-0413$07.50 © 1982 Plenum Publishing Corporation

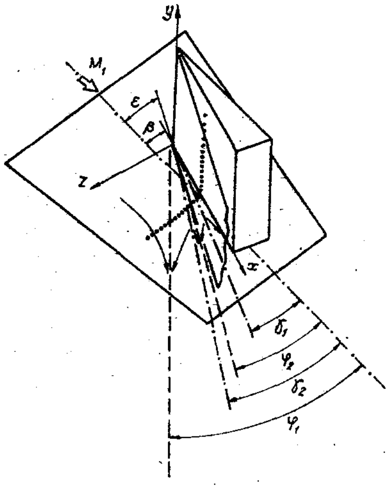

Fig. 1

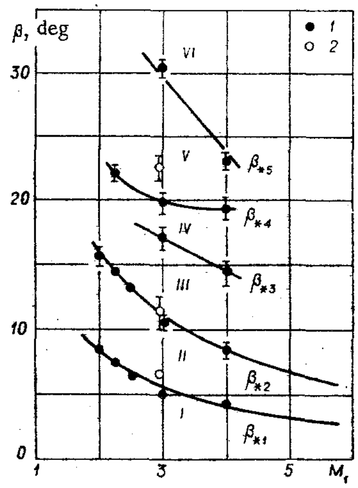

Fig. 2

bers $M_1 = 2, 2.25, 2.5, 3, 4$, unit Reynolds numbers $Re_1 = (30\text{-}36) \cdot 10^6\ m^{-1}$ and angles of shock generator deflection $\beta = 0\text{-}31°$. The wedge is rotated because of the rotation of the mobile part of the plate, executed in the form of a circle, on which it is mounted. The minimal angle of rotation assured by the measurement accuracy was 0.1° in the whole range of variation of β. The side face of the wedge and the mobile part of the plate were drained in a normal control section, at a range of 122.5 mm from the wedge leading edge. The distance from the plate leading edge to the control section at $\beta = 0$ was 430 mm. The wedge altitude is 220 mm and the length of the base is 242 mm. A wire turbulizer 0.5 mm in diameter, mounted at a distance of 3 mm from the leading edge, was used to turbulize the boundary layer on the plate. In addition to measuring the pressure distribution in the control section in the experiments, patterns of the limit streamlines on the model surface were investigated, which had been obtained by using the method of oil–soot visualization. Angles of deflection φ_1 and γ_1 relative to the unperturbed stream direction of the runoff (separation) and spreading (attachment) fundamental lines, respectively were hence determined (see Fig. 1), as were also analogous angles φ_2 and γ_2 of the secondary runoff and spreading lines for corresponding compression shock angles ε.

In contrast to the main mass of similar investigations, enclosing a narrower range of shock intensity variation, it is detected that for the case under consideration six, rather than three, fundamental interaction regimes are characteristic (see Fig. 2). In addition to the known three (I interaction without boundary layer separation; II, interaction with separation; III, flow with secondary separation), the boundaries of domains, noted earlier in [9], are determined which characterize the phenomenon of the secondary separation reversal in attenuation (domain IV), disappearance (domain V), and repeated origination (domain VI) of the secondary separation. In addition to the results obtained (the points 1), experimental data (the points 2) from [7], where conditions have been achieved corresponding to domain V and the fact of the disappearance of the secondary separation is confirmed, are presented for comparison. The boundaries of the detected domains are characterized by appropriate critical values of the angle β_*. The quantities β_{*1} and β_{*2} (in radians) are determined by relationships $M_1 \beta_{*1} = 0.3$ and $M_1 \beta_{*2} = 0.6$, proposed in [3, 4].

Going over to an analysis of the limit streamlines, obtained by using the oil–soot visualization method, which correspond to the new interaction regimes detected (Fig. 3), it should be noted that the characteristic schemes (domains I, II, III in Fig. 2), known earlier, have been examined in [1, 2, 4, 6, 9]. Only in [7, 8] have the singularities of certain new modes to be discussed in the example of the flow around a dihedral angle for $M_1 = 2.95$ and a sufficiently high Reynolds number ($Re_1 = 16 \cdot 10^7\ m^{-1}$) been also analyzed here. In contrast to the papers mentioned, a different nature of secondary separation development was observed for $\beta_{*2} \le \beta \le \beta_{*3}$ in the investigations performed, as the Mach number changes. The scheme corresponding to this regime (see Fig. 1) is qualitatively analogous to that presented in Fig. 3d and is just characterized by a rather more significant angle φ_2 of the secondary runoff (separation) line C_2 relative to the unperturbed stream direction as compared with the compression shock (CS) angle ε. For $M_1 = 3$ and 4 the secondary runoff C_2 and spreading P_2 lines (Fig. 3d) were formed by reaching $\beta = \beta_{*2}$ practically at one over the whole length of the interaction domain. At the same time, a gradual increase in the extent of these lines was observed with the growth of β in the case $M_1 = 2$, as occurred in the investigations mentioned earlier that were performed for higher Reynolds numbers. In conformity with the representations elucidated in these papers, the detected action of the

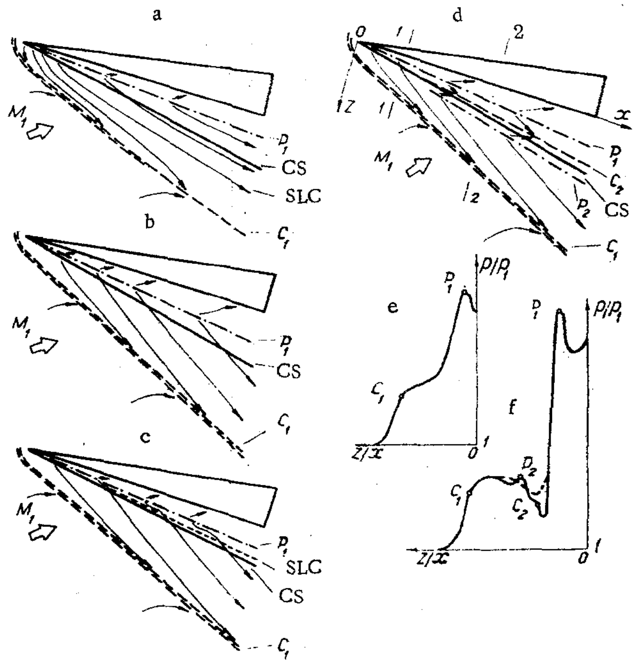

Fig. 3

Mach number on the nature of secondary separation development is completely explainable by the influence of a different boundary layer state in the separation zone in the reverse flow domain between P_1 and C_1, which is determined by the extent of the limit streamlines for a fixed single Reynolds number, i.e., the local Reynolds number. It can be assumed that because of the sufficiently low single Reynolds number that existed in the experiments performed, the boundary layer was everywhere laminar for $M_1 = 3$ and 4 in the domain of secondary separation formulation. A diminution of the Mach number to $M_1 = 2$ involved an increase in the shock angle ε and the extent of the separation zone (the angles of deflection φ_1 and φ_2, respectively, of the runoff lines C_1 and C_2). Consequently, the boundary layer made the transition into the turbulent state in the domain of sufficiently high local Reynolds numbers, and the positive pressure gradient between the lines C_2 and P_2, which is realized in the reverse flow direction, turned out to be insufficient to cause secondary separation. The absence of the lines C_2 and P_2 in the neighborhood of the leading edge of the shock generator (see Fig. 3d) is evidently related to the fact that, according to [10], no positive pressure gradient occurs in the domain between P_1 and C_1 in the reverse flow direction, which indicates the essentially three-dimensional nature of the flow therein. The appropriate pressure distribution in the characteristic section 1–1 (see Fig. 3d) is presented in Fig. 3e. At the same time, the separation flow becomes quasiconical with distance from the edge of the generator.

As the investigations performed showed, increasing the angle β in the range $\beta_{*2} \leq \beta < \beta_{*3}$ (see Fig. 2) is accompanied by further magnification of the secondary separation criteria. However, for $\beta_{*3} \leq \beta < \beta_{*4}$ a certain attenuation in the secondary runoff and spreading lines is observed. In connection with the complexity of fixing the beginning of this regime, the boundary corresponding to $\beta = \beta_{*3}$ (see Fig. 2) is determined to not more than $\pm 1°$ accuracy. For certain $\beta > \beta_{*3}$ (see Fig. 3a) these secondary lines become practically indistinguishable; however, the limiting separating streamline (SSL) above which the flow deviates in a direction to C_1, and below which does not reach C_1, can still be isolated. In addition, starting with certain values of $\beta > \beta_{*3}$, bifurcation of the runoff line C_1 is detected in a finite section of the flow from the edge of the shock generator, whose extent increases as β grows further (see fig. 3a–d). An analogous phenomenon was noted earlier in [10]. The behavior of the limit streamlines between the two runoff lines being formed is sufficiently complex to establish because of the strong blurring of the oil–spot mixture.

Upon reaching the value $\beta = \beta_{*4}$ the complete disappearance of secondary separation is observed (see Fig. 3b), and a further increase in β in the range $\beta_{*4} \leq \beta < \beta_{*5}$ is characterized by its absence. For $\beta = \beta_{*5}$ repeated curvature of the streamline (SLC) is detected in the reverse flow region (see Fig. 3d), indicating the generation of secondary separation. A flow with clearly defined secondary separation criteria corresponds to the values $\beta > \beta_{*5}$ (see Fig. 3d). Detailed measurement of the pressure distribution on the surface at the section 2–2 permitted the detection of an additional singularity in the neighborhood of the secondary separation zone for this regime (see Fig. 3f, solid line) as compared with that typical for smaller values of the angle β (dashed line). The maximum in the neighborhood of the line P_2 and the region of the pressure plateau being formed between the lines C_2 and P_2 are remarkable. An analogous nature for the pressure distribution in the secondary separation region was observed in [11] during flow by an opposite near-wall jet being ejected into a supersonic stream. Taking account of the results of this paper, it can apparently be assumed that for $\beta > \beta_{*5}$ the internal shock originating in supersonic reverse flow will be transformed into a λ-configuration of shocks, as above the main separation zone. As the measurements executed showed, for $\beta > \beta_{*5}$ the maximum pressure on the line P_2 practically equals the pressure in the region of the main separation zone plateau p_p or can even exceed it somewhat for sufficiently large β.

It is very important that, in conformity with the investigations performed, the repeated origination of the secondary separation over the whole length of the interaction domain simultaneously for different numbers M_1 be fixed approximately for the very same critical ratio between the pressure on the line P_2 (see Fig. 3f) and the minimal pressure between the lines P_1 and C_2 ($\xi_{*5} \approx 1.5$). The boundary corresponding to this value is denoted by the solid line for $\beta = \beta_{*5}$ (see Fig. 2). Therefore, the quantity ξ_{*5} characterizing the intensity of the local shock originating in the reverse flow agrees with the critical intensity $\xi_{*1} = 1.5$ of the oblique shock initiating the separation flow for $\beta = \beta_{*1}$ and, according to [3], corresponds to the conditions for three-dimensional separation of a boundary layer in the turbulent state. This affords a foundation for the assumption that the cause of the disappearance of secondary separation in the domain V (see Fig. 2) is in addition to the necessary condition noted earlier: The conical supersonic nature of the reverse flow can apparently be the acceleration, due to different factors, of the boundary layer transition into the turbulent state in the separation zone as β grows when $\beta \geq \beta_{*4}$. One such factor, for example, is the growing positive pressure gradient in the reverse flow, whose action under sub- and supersonic flow condition is probably distinct. The lack of systematic data about the critical intensity of a compression shock, corresponding to the separation condition in the laminar boundary layer situation under consideration, does not, unfortunately, permit exact estimates to be made about the possibility of the existence of a secondary separation flow for $\beta = \beta_{*4}$ in case the return flow were to be laminar. Refinement of this question requires further investigation.

According to the data obtained (see Fig. 2), an increase in the number M_1 is accompanied by a diminution in the extent of the domain of secondary separation disappearance V, and for $M_1 \sim 4.5$-5 this domain should be missing. Indeed, results presented in [1] confirm the existence of secondary separation for the number $M_1 = 6$ up to the value $\beta = 20°$, and its disappearance is not noted here. This can apparently be related to both the diminution in the local Reynolds numbers in the domain of secondary separation formation, and the laminar reverse flow section corresponding to the tightening, and to the more significant unfavorable pressure gradients which occur, other conditions being equal, in a reverse flow as the number M_1 increases.

Therefore, the experimental investigations performed permit refinement of the boundary for the existence of regimes, known and clarified earlier, for the three-dimensional interaction between an oblique compression shock and a turbulent boundary layer. In addition, the reasons for the secondary separation attenuation being observed in the domain IV as $\beta > \beta_{*3}$ (see Fig. 2) remain unclear. It must be noted that the existence of such a domain is not determined in analogous investigations [7, 8], performed for $M_1 = 2.95$ and sufficiently high Reynolds numbers. Only a hypothesis relative to the probable causes can be proposed for the different flow development being observed in the separation zone. For example, the substantial influence of the single Reynolds number on the development of the boundary layer transition from the laminar to the turbulent state on a plate as the stream velocity changes is known [12-14]. It is possible that an analogous influence on transition in the separation zone during the increase in return flow velocity as the shock intensity grows will determine the different nature of secondary separation formation for substantially distinctive Reynolds numbers. It can also be assumed that the model configuration also exerts a definite influnece on this process. Thus, in the case of flow in a dihedral angle the compression shock interacts with the laminar and transition boundary layer in the neighborhood of the leading edge. It is possible that the effects of this interaction, being propagated along the stream, will also exert influence on secondary separation development. The exact explanation of the singularity noted above is associated with the necessity for further systematic investigations.

In connection with the known difficulties of a theoretical analysis of the separation flows under consideration, generalizations of their different characteristics in order to obtain correlation relations acquire special importance. Systematic investigations performed, as well as generalizations of extensive, known experimental results permit the proposal of an approximate method for computing the pressure distribution in the neighborhood of such separation zones for different situations of separation formation: in the presence of a turbulent boundary layer on the surface ahead of the shock generator and without it, for instance, in the flow around a dihedral angle with intersecting leading edges in the case of large Reynolds numbers.

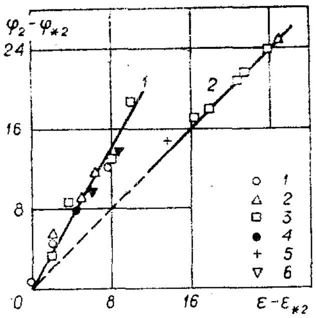

Fig. 4

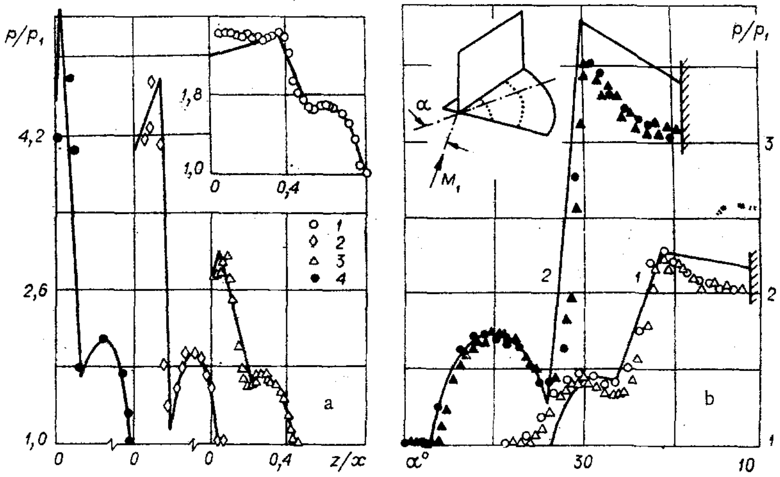

Fig. 5

According to [4, 9], the angles of deflection φ_1 and γ_1 of the runoff C_1 and spreading P_1 lines relative to the unperturbed stream direction are determined by the relationships $\varphi_1 - \varphi_{*1} = 1.82(\varepsilon - \varepsilon_{*1})$ and $\gamma_1 - \gamma_{*1} = 1.17(\varepsilon - \varepsilon_{*1})$, where $\varphi_{*1} = \varepsilon_{*1}$ as well as γ_{*1} correspond to $\beta = \beta_{*1}$ and depend on the number M_1. The experimental data for the angle φ_2 of the secondary runoff line C_2 are generalized in an analogous manner (Fig. 4: 1-3 for $M_1 = 2.25$, 3.0, 4.0, respectively, in this paper; 4 for 2.5; 5 for 5.9 from [1]; 6 for 2.95 from [7]). In the subsonic transverse flow domain, the dependence $\varphi_2 - \varphi_{*2} = 1.72(\varepsilon - \varepsilon_{*2})$ (line 1) is valid in the separation zone, where $\varphi_{*2} = \varepsilon_{*2}$ corresponds to $\beta = \beta_{*2}$, while for the supersonic flow the dependence $\varphi_2 = \varepsilon$ (line 2) is valid. Taking account of the known relationship for the oblique shock intensity $\xi = [2\varkappa/(\varkappa+1)](M_1 \sin\varepsilon)^2 - (\varkappa - 1)/(\varkappa + 1)$, where $\varkappa = 1.4$, and also the equality $\xi_{*1} = 1.5$ [3], we can obtain $\varepsilon_{*1} = \sin^{-1}(1.195/M_1)$. Analogously, a consequence of the equality $\xi_{*2} = 2.2$ detected in the considered Mach number range for $\beta = \beta_{*2}$ is $\varepsilon_{*2} = \sin^{-1}(1.424/M_1)$. The relationships considered above permit more convenient dependences to be obtained which will determine the angles of deflection of the runoff C_1 and spreading P_1 lines:

$$\varphi_1 = 1.82\varepsilon - 0.82 \arcsin(1.195/M_1); \tag{1}$$

$$\gamma_1 = \begin{cases} 1.17\varepsilon - 0.85 \arcsin(1.195/M_1) & \text{at} \quad \delta \neq 0, \\ 1.17\varepsilon - 0.498 \arcsin(1.195/M_1) & \text{at} \quad \delta = 0. \end{cases} \tag{2}$$

Condition (2) is obtained when taking into account that $\gamma_{*1}/\varepsilon_{*1} = 0.32$ in the Mach number range under consideration when a boundary layer with thickness $\delta \neq 0$ exists in the neighborhood of the shock generator leading edge, while $\gamma_{*1}/\varepsilon_{*1} = 0.682$ for $\delta = 0$ [9].

A number of characteristic points can be extracted in describing the pressure distribution in a certain section $x = \text{const}$ in the quasiconical flow domain in the case $\beta < \beta_{*5}$, as the relative coordinate z/x increases. The qualitative nature of the pressure distribution is presented in Fig. 3f for such situations (the curve with the section denoted by dashes). According to the generalizations made, the relative pressure $z/x = 0$ is

$$p/p_1 \approx \xi. \tag{3}$$

As z/x increases to the value $(z/x)_1 = \tan(\gamma_1 - \beta)$ corresponding to the spreading line P_1, the pressure rise is assumed linear to the quantity

$$p/p_1 = \begin{cases} 1.48(M_1 \sin\varepsilon)^2 - 0{,}617 & \text{at} \quad \beta \geqslant \beta_{*1}, \\ \xi & \text{at} \quad \beta < \beta_{*1}. \end{cases} \tag{4}$$

The subsequent diminution of the pressure for $z/x > (z/x)_1$ to a certain point corresponding to its minimum can also be considered linear. The angle ψ of the line of mentioned minimal values is determined by the relationship $(\psi - \beta)/(\varepsilon - \beta) = 0.9$ [9], and therefore, the coordinate of a point on this line is $(z/x)_2 = \tan[0.9(\varepsilon - \beta)]$. On the basis of the generalized experimental data [9], the dependence

$$p/p_1 = 1 + (p_p/p_1 - 1)[1 - |(z_* - 0.64)/0.46|^3], \tag{5}$$

is obtained to describe the pressure distribution in the separation zone from the point of the beginning of its rise to the minimum point noted, where $z_* = [(z/x) - (z/x)_1]/[(z/x)_3 - (z/x_1)]$, and $(z/x)_3$ is the coordinate of a point on the runoff line C_1 determined by the relationship

$$(z/x)_3 = \mathrm{tg}(\varphi_1 - \beta) + (2.85\delta/x)\{1 - [(\beta - \beta_{*1} - 15)/15]^2\} \tag{6}$$

(β in degrees). Because of the existing analogy between two- and three-dimensional separation flows [2, 4], the relative pressure in the region of the plateau p_p/p_1 can here be calculated sufficiently exactly by any of the known valid relations for two-dimensional separation flows including $M_n = M_1 \sin \varepsilon$ or $M_n = M_1 \sin \varphi_1$ [7, 8].

The computations presented in the proposed method for the different conditions of separation flow formation and wide range of β and M_1 variation illustrate the satisfactory agreement with results of experiments (Fig. 5a, ($\delta = 0$): 1) $M_1 = 2.0$, $\beta = 14.4°$, 2) $M_1 = 4.03$, $\beta = 16.3°$ – [15]; ($\delta \neq 0$): 3) $M_1 = 3.71$, $\beta = 12°$ – [10]; 4) $M_1 = 5.89$, $\beta = 12°$ [16]; b) ($\delta = 0$): 1) $M_1 = 2.95$, $\beta = 11°$; 2) $\beta = 18.5°$ [7, 8]).

The author is deeply grateful to A. M. Kharitonov, V. I. Kornilov, V. A. Lebige, S. A. Gaponov, and N. F. Polyakov for discussing the research and for useful remarks.

LITERATURE CITED

1. R. K. Korkegi, "On the structure of three-dimensional shock-induced separated flow regions," AIAA J., 14, No. 5 (1976).
2. V. S. Dem'yanenko and V. A. Igumnov, "Three-dimensional shock interaction with a turbulent boundary layer in the region of interference of intersecting surfaces," Izv. Sib. Otd. Akad. Nauk SSSR, Ser. Tekh. Nauk, No. 8, Issue (1975).
3. R. H. Korkegi, "A simple correlation for incipient turbulent boundary-layer separation due to a skewed wave," AIAA J., 11, No. 11 (1973).
4. A. A. Zheltovodov, "Physical singularities and certain properties of two- and three-dimensional separation flows at supersonic velocities," Izv. Akad. Nauk SSSR, Mekh. Zhidk. Gaza, No. 3 (1979).
5. L. F. Scuderi, "Expressions for predicting three-dimensional shock wave-turbulent boundary layer interaction pressures and heating rates," AIAA Paper, No. 162 (1978).
6. B. Oskam, I. E. Vas, and S. M. Bogdonoff, "Mach 3 oblique shock wave-turbulent boundary layer interactions in three dimensions," AIAA Paper No. 336 (1976).
7. M. A. Zubin and N. A. Ostapenko, "Experimental investigation of the three-dimensional supersonic flow structure with boundary layer separation in corners," Jet and Separation Flows [in Russian], Moscow State Univ. (1979).
8. M. A. Zubin and N. A. Ostapenko, "Flow structure in the separation region during normal compression shock interaction with a boundary layer in a corner," Izv. Akad. Nauk SSSR, Mekh. Zhidk. Gaza, No. 3 (1979).
9. A. A. Zheltovodov, "Three-dimensional interaction of a compression shock generated by a wedge obstacle and a turbulent boundary layer," Aerophysical Studies [in Russian], No. 6, ITPM Sib. Otd. Akad. Nauk SSSR, Novosibirsk (1976).
10. R. D. Neumann and K. H. Token, "Prediction of surface phenomena induced by three-dimensional interactions on planar turbulent boundary layers," 25th Congress, Pap. No. 74-058, Amsterdam (1974).
11. A. I. Glagolev and Yu. A. Panov, "Investigation of the escape of opposing near-wall jets into a supersonic stream from an obstacle on a plate surface," Jet and Separation Flows [in Russian], Moscow State Univ. (1979).
12. N. F. Polyakov, "Laminar boundary layer under conditions of a 'natural' transition to turbulent flow," Development of Perturbations in a Boundary Layer [in Russian], ITPM Sib. Otd. Akad. Nauk SSSR, Novosibirsk (1979).
13. A. M. Kharitonov, "Influence of stream perturbations on laminar to turbulent boundary layer transition," in: Aeromechanics [in Russian], Nauka, Moscow (1976).
14. S. A. Gaponov and A. A. Maslov, Perturbation Development in Compressible Flows [in Russian], Nauka, Novosibirsk (1980).
15. V. S. Dem'yanenko, "Experimental investigation of three-dimensional supersonic gas flows in the interaction surface interference domain," Candidate's Dissertation, Technical Sciences, ITPM Sib. Otd. Akad. Nauk SSSR (1973).
16. R. G. Christophel, W. A. Rockwell, and R. D. Neumann, "Tabulated Mach-6 three-dimensional shock wave-turbulent boundary layer interaction heat transfer data," AFFDL-TM-74-212-FXG Supplement, Air Force Flight Dynamics Laboratory (February, 1975).